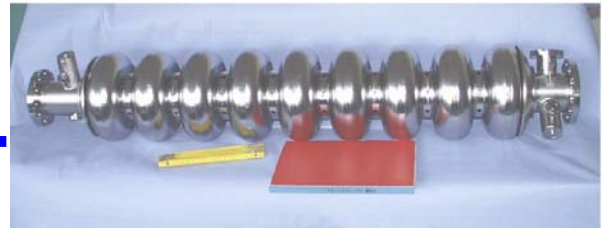




# SRF



## **RRR OF COPPER COATING AND LOW TEMPERATURE ELECTRICAL RESISTIVITY OF MATERIAL FOR TTF COUPLERS**

M. Fouaidy, N. Hammoudi, IPN Orsay, France  
S. Prat, LAL, France

### **Abstract**

In the frame of the R&D program on the TTF III main RF coupler, IPN Orsay developed in close collaboration with LAL institute, a dedicated facility for the electrical characterization of different materials at low temperature. This apparatus was used for measuring the electrical resistivity versus temperature (4.2 K- 300K) of various samples produced in the industry. These tests were performed in order to compare the RRR of the samples, qualify and find the optimum parameters for the coating process. Seven flat samples were tested in a saturated liquid helium bath under ~1013 mBar pressure: measurements were performed on bare 316L samples, nickel coated 316L samples, copper coated 316L samples with a nickel under layer. We investigated, in particular, the effect of vacuum annealing at 400°C on the RRR of the copper coating. Our experimental data are compared to previous results reported by other groups, empirical correlation and a good agreement was found. Finally, the tested samples fulfil the TTF III design parameters requirements in terms of heat loads to the refrigerator at 2 K, 4 K and 70 K.

Contribution to the SRF 2005, Ithaca, New York, USA

Work supported by the European Community-Research Infrastructure Activity under the FP6 “Structuring the European Research Area” programme (CARE, contract number RII3-CT-2003-506395).

## RRR OF COPPER COATING AND LOW TEMPERATURE ELECTRICAL RESISTIVITY OF MATERIAL FOR TTF COUPLERS

M. Fouaidy, N. Hammoudi, IPN Orsay, France  
S. Prat, LAL, France

### Abstract

In the frame of the R&D program on the TTF III main RF coupler, IPN Orsay developed in close collaboration with LAL institute, a dedicated facility for the electrical characterization of different materials at low temperature. This apparatus was used for measuring the electrical resistivity versus temperature (4.2 K- 300K) of various samples produced in the industry. These tests were performed in order to compare the RRR of the samples, qualify and find the optimum parameters for the coating process. Seven flat samples were tested in a saturated liquid helium bath under  $\sim 1013$  mBar pressure: measurements were performed on bare 316L samples, nickel coated 316L samples, copper coated 316L samples with a nickel under layer. We investigated, in particular, the effect of vacuum annealing at  $400^\circ\text{C}$  on the RRR of the copper coating. Our experimental data are compared to previous results reported by other groups, empirical correlation and a good agreement was found. Finally, the tested samples fulfil the TTF III design parameters requirements in terms of heat loads to the refrigerator at 2 K, 4 K and 70 K.

### INTRODUCTION

The power coupler is a crucial component for operating superconducting RF cavities. The main function of this device is the efficient transfer in matched condition of the RF power from the RF source to the particles beam. This complex device operates in stringent conditions: 1) it should handle and transmit a high RF power ( $\sim 250$  kW-500 kW) through a ceramic window, 2) it is an interface between parts of the accelerating cryomodule at room temperature and cryogenic temperatures, 3) it is also an interface between atmospheric pressure in the wave guide operating at room temperature and ultrahigh vacuum ( $<10^{-8}$  mBar) in the SRF cavity. Due to such operating conditions, the RF power coupler should be carefully designed in order to achieve reliably the required performance. For a large superconducting linac such as ILC or XFEL, it is mandatory to minimize the cryogenic power needed for the machine. Consequently, the static and dynamic heat load contribution of the RF power coupler to the cryomodule must be kept as low as possible. In the frame of CARE-SRF project WP7 supported by EU, LAL and DESY laboratories launched an R&D program aimed at development and fabrication in the industry of thirty TTF III power couplers [1]. In this program, the development of high performance copper coating for the different parts of the power coupler

is of prime importance for reducing the cryogenic thermal budget to the refrigerator operating at a  $T=2$  K.

### MAIN DESIGN PARAMETERS OF TTF3 COUPLER AND THERMAL SPECIFICATIONS

The TTF III power coupler (Fig. 1) is of a coaxial type with two cylindrical alumina windows: 1) a warm window located at the waveguide to coax transition (upper part) and operating at  $T\approx 300$  K, 2) a cold window, located at the lower part and thermally anchored to the infrared radiation shield at  $T\approx 70$  K.

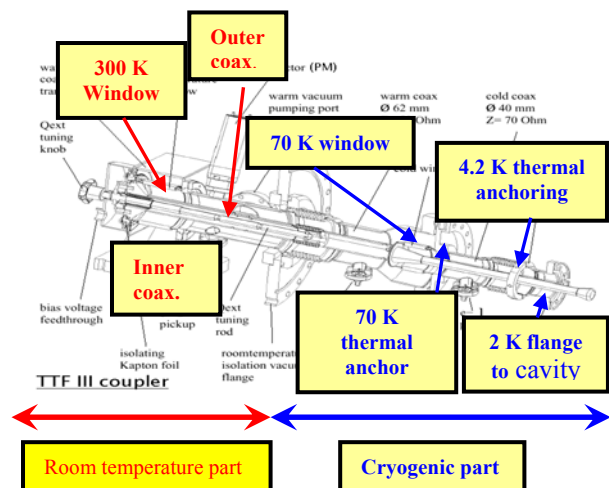


Fig. 1: Drawing of the TTF III power coupler

The inner and outer conductors are made of 316L stainless steel with copper plating (see next section) while the antenna is made of OFHC bulk copper. Furthermore, copper plated stainless steel bellows are used to avoid mechanical stresses due to differential thermal contraction between the different materials during cool down to cryogenic temperatures. Moreover, two thermal anchoring linked to infrared thermal radiations shields at 4.2 K and 70 K respectively allows the interception of the heat flux (solid conduction and RF losses (Joule heating)), hence reducing the heat load to the cavity operating at  $T=2$  K. The TTF III power coupler, operating in pulsed mode, should handle and transmit efficiently a high RF power (e.g. Peak RF power of 250 kW and an average power of 3.2 kW with a pulse length of 1300ms) to the beam with minimized heat loads to the different cooling circuits of the refrigerator ( $T=2$  K,  $T=4.2$  K and  $T=70$  K). The main design parameters, which are

important for the thermal performance of the power coupler and cryomodule, are illustrated in Table 1.

Table 1: Main design parameters of TTF III coupler and thermal specifications

Parameter	Specification
Frequency (MHz)	<b>1300</b>
Operating mode	<b>Pulsed, total pulse length : <math>\tau_p=1300</math> <math>\mu</math>s, rise time <math>\tau_R=500</math> <math>\mu</math>s, flat top with beam <math>\tau_{FTop}=800</math> <math>\mu</math>s</b>
Heat load @ 2 K (mW)	<b>60</b>
Heat load @ 4 K (mW)	<b>500</b>
Heat load @ 70 K (W)	<b>6</b>
Peak RF power (kW)	<b>250</b>
Average RF power (kW)	<b>3.2</b>
Repetition rate (Hz)	<b>10</b>

### Copper coating specifications for the TTF-3 couplers

Among others items, the copper coating of different parts of the coupler is an important task in order to achieve the required RF and thermal performance. The optimum values of the coating characteristics (thickness  $e_{Cu}$ , purity, low hydrogen content, residual electrical resistivity  $\rho_R$ , low temperature thermal conductivity  $k_{Cu}(T)$ , low temperature surface resistance  $R_S(T)$ , adhesion on stainless steel substrate and surface roughness  $R_a$ ) are a compromise between several criteria. More precisely, the heat load  $Q_{Cold}$  to the 2 K circuit should be minimum and have two contributions, namely the static part  $Q_{cond}$  and the dynamic part  $Q_{RF}$ . The static part is due to solid conduction and is simply given by the expression:

$$Q_{cond} = \frac{A_{Cu}}{L_{eff}} \int_{TC}^{TH} k_{Cu}(T) \cdot dT \quad (1)$$

With:

- $A_{Cu}$  : area of the copper coating in the heat flow direction ( $A_{Cu} \cong \pi \cdot D_{eff} \cdot e_{Cu}$ ),
- $D_{eff}$  : effective diameter of the coated substrate (pipe or bellow),
- $L_{eff}$  : effective length of the conduction thermal path,
- TC cold temperature,
- TH hot temperature.

The dynamic part  $Q_{RF}$  is due to Joule heating of the copper coating by the RF surface magnetic field  $H_S$ :

$$Q_{RF} = \frac{1}{2} \iint_{SCu} R_S(T) \cdot H_S^2 dS \quad (2)$$

From the above relation ship (1), the conduction heat flux  $Q_{Cold}$  is proportional to both the thickness and the thermal conductivity of the copper coating ( $Q_{cond} \propto A_{Cu} \cdot k_{Cu} \propto e_{Cu} \cdot k_{Cu}$ ). Then to reduce  $Q_{Cold}$ ,  $k_{Cu}$  should be lowered (i.e. the purity should be low) as well as the thickness. On the contrary to reduce the RF losses  $Q_{RF}$ ,  $R_S(T)$  should be decreased: 1) in the normal skin effect regime the low temperature surface resistance  $R_{S0}$  is proportional to the square root of the residual DC resistivity (e.g.  $R_{S0} \propto (\rho_R)^{0.5}$ ), hence  $\rho_R$  should be minimum namely copper purity should be high, 2) in the anomalous skin effect regime the low temperature surface resistance  $R_{S0}$  is independent of copper purity or  $\rho_R$  (for copper at TESLA frequency  $f=1300$  MHz,  $R_{S0}=1.3$  m $\Omega$ ). Now it is clear that the two previous criteria are contradictory: more precisely to reduce  $Q_{cond}$  (respectively  $Q_{RF}$ ) we should use low purity (respectively high purity) copper coating. As these two criteria go to reverse direction, there is an optimum value of  $\rho_R$  or coating RRR (Residual Resistivity Ratio). The RRR is defined as the ratio of the room temperature ( $T \cong 300$  K) electrical resistivity to the residual electrical resistivity  $\rho_R$  measured at the Lhe normal boiling point ( $T=4.22$  K):

$$RRR = \frac{\rho(T = 273K)}{\rho_R} \cong \frac{\rho(T = 300K)}{\rho_R} \quad (3)$$

The following specifications and preparation procedure of the copper coatings are needed to achieve reliably the required RF and thermal performance (Table 1) of the TTF III power coupler:

- 1) Copper coated stainless steel is of austenitic grade AISI 316L (EN 1.4435),
- 2) Stainless steel parts are Hydrogen degassed at 950° C for 2 hours,
- 3) Thicknesses are respectively 30  $\mu$ m  $\pm$  10 $\mu$ m for the Internal Conductor (IC) and 10  $\mu$ m  $\pm$  5 $\mu$ m for the Outer Conductor (OC) coating as specified in the drawings,
- 4) Sufficient adhesion of the copper on pipes and bellows,
- 5) Low hydrogen content,
- 6) Surface roughness  $R_a < 1.6$   $\mu$ m
- 7) Ni flash under layer thickness  $\leq 1$   $\mu$ m
- 8) Electrical resistivity:  $RRR \geq 30$  after baking at 400°C during 1 h in a vacuum furnace.

The effect of copper coating RRR on the heat loads at cryogenic temperature [2] for the three thermal intercepts are presented in Table 2. The results of Table 2 clearly show that a RRR of the copper coating higher than 30 fulfils the required thermal performance at 2 K and 4 K with a sufficient safety margin

Table 2: Effect of the copper coating RRR on the heat loads at cryogenic temperature for the three thermal intercepts.

Thick. (μm)	Conduc.	RRR	Load @2K (mW)	Load @ 4K (mW)	Load @ 70 K (W)
10	IC	10	70	500	9.6
30	OC	10	70	500	9.6
10	IC	100	110	600	9.2
30	OC	100	110	600	9.2

## COPPER COATING TECHNIQUE AND ROOM TEMPERATURE CHARACTERIZATION OF SAMPLES

Two main techniques could be used for coating stainless substrate with high purity copper: a) electrolytic deposition, b) magnetron sputtering. In our case, we have chosen the first method because, as compared to the second one, it allows the production of high material performance and better coating in much easier manner. Briefly, the electrolytic coating process is performed in bath which contains typically the following impurities:

- Chromium: 0.04 ppm,
- Cobalt < 0.04 ppm (detection limit),
- Iron: 21.8 ppm,
- Manganese: 0.01 ppm (detection limit).

The different steps of test program for the copper coating are:

- Measurements of copper RRR (flat Cu plated samples) before and after 400° C baking,
- Adhesion tested on flat samples and on bellows,
- Thickness uniformity and roughness measurements on flat samples,
- Thickness uniformity and roughness are measured on bellows and pipe samples.

### Copper coating thickness measurement and micrographs

As stated above, the coating thickness is an important parameter of the material. Non destructive measurements of thickness profiles were performed by X-Ray fluorescence method. **Fischerscope**® XRAY XDL device was for that purpose. Five copper coated samples with a specified thickness  $e_{Cu} = 30 \mu m$  were tested (Fig.2). These data show that: a) the mean value of coating thickness is  $\langle e_{Cu} \rangle = 33.68 \mu m$  with a standard deviation

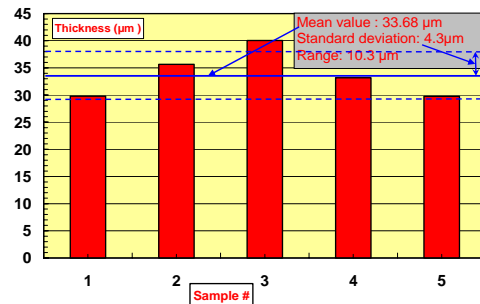


Fig. 2: Histogram of the thickness measured by X-Ray fluorescence.

$\sigma_{e_{Cu}} = 4.3 \mu m$  and a range of  $10.3 \mu m$ , b)  $\sigma_{e_{Cu}}$  is within the lower limit of the specified tolerance of  $\pm 20\%$  (i.e.  $\pm 6 \mu m$ ). Note that, out of the five samples tested, only one sample (#3) is outside the lower tolerance limit. Moreover, the micrographs illustrating the copper coating thickness distribution of the bellows is shown in Fig.3. The measured values  $28 \mu m$  -  $34 \mu m$  are well in the specification range ( $30 \mu m \pm 10 \mu m$ ).

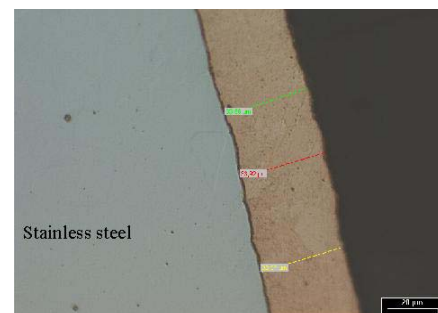


Fig. 3: Copper coating thickness distribution in some locations of the small bellows.

### Analysis of copper coating surface and impurities

Samples were cut out from the copper coated bellows and the copper coating surfaces were analysed using EBM (Fig. 4).

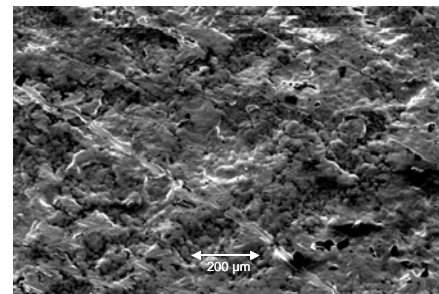


Fig. 4: Electron-Beam microscope (EBM) image of a Cu coated sample

In order to determine the impurities content of the copper coating, we performed spectrum analysis. The recorded spectrum (Fig. 5) shows that the predominant

elements are copper (~70%) and oxygen (~30%) with traces of carbon, iron and nickel.

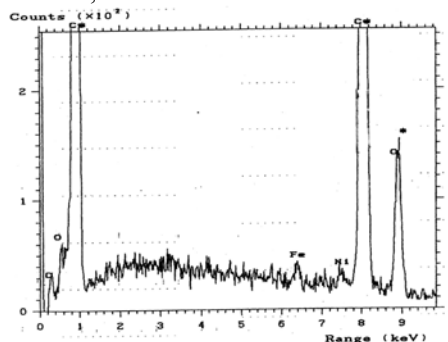


Fig.5: Spectrum of a sample for elemental analysis of the copper coating.

### Copper coating parts of TTF3 coupler

The copper coating characteristics produced in the industry achieved the required properties (see next section for RRR results) so we decided to coat the different parts of the TTF3 coupler (Fig.6).



Fig. 6: Photographs of the different copper-plated parts of TTF3 coupler

## ELECTRICAL RESISTIVITY AND RRR MEASUREMENT

### Experimental set-up and procedure

The measurements were performed using the standard DC 4 probes method (Fig. 7). The electrodes are clamped to the flat sample by means of copper-beryllium springs:

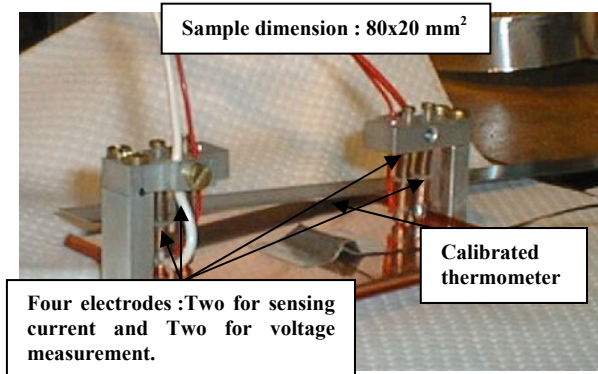


Fig. 7: A) Double side copper plated (30  $\mu\text{m}/\text{side}$ ) 316L type stainless steel sample.

the resulting contact pressure between the electrodes tips and the sample is ~12 Bars. A Kapton foil of ~0.1 mm thickness is used for electrical insulation between the sample and electrodes support. Note that the distance between the voltage electrodes is ~60 mm. The test-sample, which is equipped with a calibrated CERNOX thermometer ( $T=1.6\text{K} - 300\text{K}$ ), is then immersed in a saturated liquid helium bath (Pressure:  $P=100\text{ kPa}$ , Temperature  $T=4.2\text{ K}$ ). The sensing current (precise standard DC voltage supply SODILEC) is set to a value ~1.5 A, is maintained constant during the whole test and on-line measured via the voltage drop across a precision resistor ( $R=1\ \Omega$ ,  $\Delta R/R \sim 10^{-4}$ ).

The experimental procedure is the following:

- Perform 10 measurements at  $T=4.2\text{ K}$ , each measurement consisting of 15 dual scans in the direct (+V) and reverse direction (-V),
- Vaporize the liquid helium using a bath heater,
- Heat the sample in a controlled way to maintain it at a given constant temperature  $T$  in the range  $4.2\text{ K} - 300\text{ K}$ ,
- Once  $T$  is stable, perform 10 measurements (5 to 10 dual scans),
- This procedure (c-d) is repeated as function of temperature from  $4.2\text{ K}$  to  $300\text{ K}$ .

Note that, as the measured signal is very small (i.e.  $45\ \mu\text{V} - 450\ \mu\text{V}$ ), the change of the sensing current direction is mandatory in order to eliminate parasitic thermal voltages.

### Results and discussion

Due to the very low thickness (~10-30  $\mu\text{m}$ ) of the copper coating and the electrical contact type between sample and measuring electrodes (no soldering, contact by pressure), it is not possible to measure directly the resistance of the copper coating alone and especially at cryogenic temperatures: the sample could be broken. Moreover, the coating electrical resistivity should be measured in real operating conditions (i.e. with the stainless steel substrate): the coating mechanical stress has an influence on the electrical resistivity. Consequently, the measurement method is by comparison: we should measure both coated and uncoated samples including those with only the nickel under layer coating, which is sandwiched between stainless steel substrate and the copper coating. Further, in our knowledge, only few precise results of the electrical resistivity of Stainless Steel (SS) at low temperature were previously published it is then interesting to get such data. Six coated and uncoated samples (Table 3) were tested. Note that for all the coated samples, the thickness of the nickel under layer is 1-2 $\mu\text{m}$ . The sample #1 was tested twice: a) as received, b) after annealing at  $400^\circ\text{C}$  in a vacuum furnace. The sample #4 was also tested twice: a) as received, b) after chemical removal of the nickel under layer.

Table 3: Description of the tested samples

Sample #	Description
1 as received	SS + Ni under layer coating+ copper coating: double sided (30µm/side)
1 after vacuum annealing (400°C, 1h00)	SS + double sided copper coating (30µm/side)
3	Bare 316L Stainless Steel
4	SS + double sided Ni under layer coating
4A	Sample #4 after chemical removal of Ni
5	SS + Ni under layer coating+ copper coating: double sided (33µm/side)
6	SS + Ni under layer coating+ copper coating: double sided (33µm/side)

The variations of the electrical resistance of the copper plated sample #1  $R_{\text{Sample},1}$  versus temperature are presented in Fig. 8. As expected, these data show the well-known monotonic and strong decrease of  $R_{\text{Sample},1}$  with T from  $285\mu\Omega$  at 286 K down to  $31.8\mu\Omega$  at 4.2 K: this behaviour is typical of medium and high purity metals. Note that the mean measured value (10 measurements) at  $T = 4.2$  K is  $R_{\text{Sample},1} = 31.8 \mu\Omega$  with a mean standard deviation  $\sim 5 \cdot 10^{-3}$ . Furthermore, these data clearly show that the overall electrical conductance of the sample is dominated by the conductance of the copper which have a much lower electrical resistivity (factor of  $\sim 300$  at  $T = 4.2$  K) as compared to stainless steel : a) for copper of  $\text{RRR} = 10$   $\rho = 1.95 \cdot 10^{-8} \Omega \cdot \text{m}$  @ 300 K and  $\rho = 1.7 \cdot 10^{-9} \Omega \cdot \text{m}$  at 4.2 K, b) for copper with a  $\text{RRR} = 30$ ,  $\rho = 1.84 \cdot 10^{-8} \Omega \cdot \text{m}$  at  $T = 300$  K and  $\rho = 5.7 \cdot 10^{-10} \Omega \cdot \text{m}$  @ 4.2 K, c) for stainless steel  $\rho = 0.78 \cdot 10^{-6} \Omega \cdot \text{m}$  @ 300 K and  $\rho = 0.53 \cdot 10^{-6} \Omega \cdot \text{m}$  at  $T = 4.2$  K. The measured electrical resistivity versus temperature for 316 L stainless steel is shown in Fig. 9. Our data are in a very good agreement with earlier results obtained by Clark et al. [3] with four different samples. Note that Clark performed the measurements at only

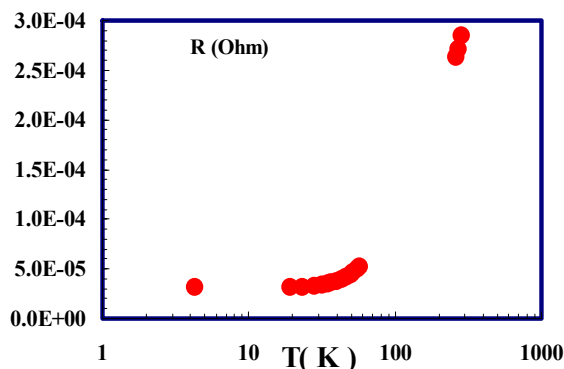


Fig. 8: Sample #1 electrical resistance versus temperature.

five fixed points, namely in ice and liquid water mixture, normal boiling points of nitrogen, hydrogen and helium respectively. Furthermore, a second stainless steel sample #4A was tested: the data obtained are close ( $\pm 8\%$ ) to those of sample #3 (Fig. 9).

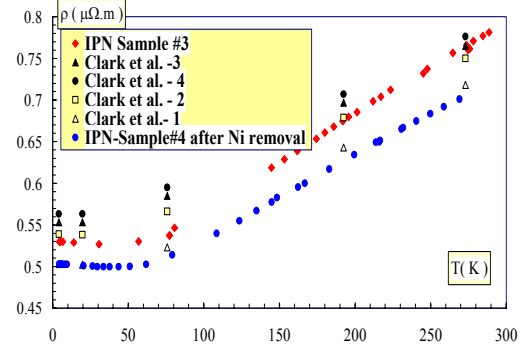


Fig. 9: Electrical resistivity of 316L type stainless steel versus temperature: comparison of IPN Orsay experimental data with previous results

The double side coated sample could be simply modelled as a network with five resistances in parallel: one for stainless steel substrate, two for copper and two for nickel. The equivalent electrical conductance of the sample is simply:

$$\frac{1}{R_{\text{Sample}}} = \frac{l}{L} \left( \frac{e_{\text{SS}}}{\rho_{\text{SS}}} + \frac{2 \cdot e_{\text{Cu}}}{\rho_{\text{Cu}}} + \frac{2 \cdot e_{\text{Ni}}}{\rho_{\text{Ni}}} \right) \quad (4)$$

Where:  $R_{\text{sample}}$  is the sample electrical resistance.  $e_{\text{SS}}$ ,  $e_{\text{Cu}}$  and  $e_{\text{Ni}}$  are the thickness of the stainless steel substrate, copper coating and nickel under layer coating respectively.  $\rho_{\text{SS}}$ ,  $\rho_{\text{Cu}}$  and  $\rho_{\text{Ni}}$  are the electrical resistivities of stainless steel substrate, copper coating and nickel under layer coating respectively. The results obtained with samples #3, # 4 and #5 are illustrated in Fig. 10. These data clearly show the effect of nickel and copper on the electrical resistance of the sample. Note that the contribution of the nickel layer to the overall resistance of the sample, thought is measurable, is small as compared to that of copper. This is simply due to 2 factors: a) the very low thickness of Ni as compared to Cu and substrate, b) the high electrical resistivity of the nickel sub layer, which is probably dirty or alloyed.

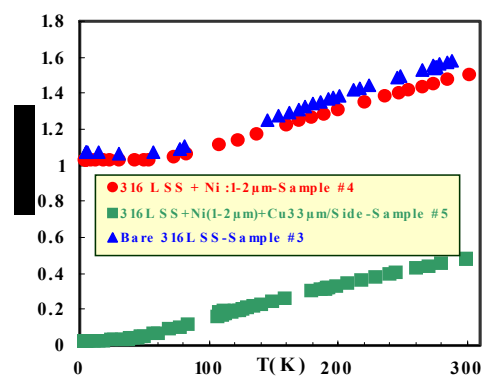


Fig.10: Effect of Ni under layer: bare stainless steel versus Ni and Ni&Cu coated samples.

Using the equation 4 and the data shown in Fig.10, we have deduced the electrical resistivity of the copper coating (Fig. 11).

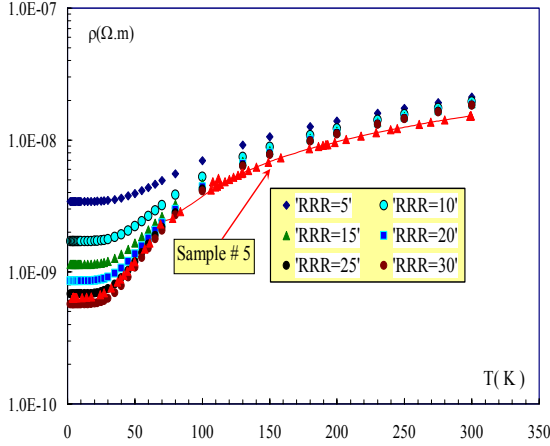


Fig. 11: Electrical resistivity of the copper coating Our data are compared to the theoretical  $\rho_{Cu}$  versus T curve which was calculated using the following empirical correlation:

$$\rho(T) = RRR \cdot \rho(273) + b \cdot \exp\left(\sum_{i=0}^{i=4} a_i \cdot (\ln(T))^i\right) \quad (5)$$

Where:  $\rho(273) = 1.7110^{-8} \Omega.m$  is the electrical resistivity of copper at the ice point temperature  $T=273$  K, b and  $a_i (0 \leq i < 4)$  are empirical constants given in the Table 4.

Table 4: Values of the empirical correlation parameters

Constant	Value
b	$10^{-8} \Omega.m$
$a_0$	-9.600976
$a_1$	-12.52445
$a_2$	8.309361

The shape of our experimental data and the theoretical curves given by expression (5) for different RRR values are similar. Moreover, the comparison of the data to the correlation lead to a theoretical  $RRR=25-30$ . Resolution of the electronics used for the tests is not sufficient for the precise measurement of the electrical resistivity of the nickel sub layer. Consequently we have to assume reasonable values of this parameter in order to deduce the RRR of copper coating from our experimental data. The summary of RRR measurements for all the samples tested are illustrated in Table 5.

For the samples without any heat treatment (i.e. as received), the RRR of Cu coating are in the range 20-46 if we use a realistic value of Ni RRR (i.e.  $RRR_{Ni} \sim 1$ ). Moreover the RRR data of sample #1 are in good agreement with the empirical correlation (5): the measured value of copper coating ( $RRR=20$ ) is consistent with that given by the correlation ( $RRR=25-30$ ).

Furthermore, the vacuum annealing at  $400^\circ C$  during one hour increases the RRR of copper coating by a factor  $\sim 6$ .

Table 5: Summary of copper coating RRR results.

Sample	Ni effect neglected	$RRR_{Ni} = 1$	$RRR_{Ni} = 300$
#1 As received	19.8	20.4	11.2
#1 Vacuum Annealed@ $400^\circ$ during 1h00	113	117	107
#5 As received	23.7	24	21
#6 As received	45.5	45.9	43

## CONCLUSION

In the frame of the CARE-SRF project WP7 R&D program aimed at development and fabrication in the industry of thirty TTF III power couplers, we designed an apparatus dedicated to the measurement of the electrical resistivity of materials at low temperatures. Several stainless steel samples coated with copper were characterized at room temperature (adhesion and thickness of the coating, impurity content, roughness...). The electrical resistivity of different materials (stainless steel, Cu coating, Ni under layer) were measured in the range 4.2 K – 300 K. The RRR of Cu coating was deduced from these data: 1) for as received samples the RRR values are in the range 20-46, 2) the vacuum annealing at  $400^\circ C$  during one hour increases the RRR of copper coating by a factor  $\sim 6$ . Moreover, our electrical resistivity data are compared to previous results reported by other groups, theoretical values, empirical correlation and a good agreement was found. Finally, the tested samples fulfil the TTF III design parameters requirements in terms of heat loads to the refrigerator at 2 K, 4 K, and 70 K.

## ACKNOWLEDGEMENTS

We acknowledge the support of the European Community-Research Infrastructure Activity under the FP6 “Structuring the European Research Area” programme (CARE, contract number RII3-CT-2003-506395)

## REFERENCES

- [1] T. Garvey et al. ‘The Tesla High Power Coupler Program at Orsay’, Proc. *SRF20003*, 8 -12 September 2003, Travemunde, German.
- [2] Dohlus M., Kostin D.Möller W.-D., ‘Tesla RF power Coupler Thermal Calculations’, Proc. of *LINAC 2004 Lübeck, Germany*, 16 - 20 August 200.
- [3] A. F. Clark et al., *Cryogenics*, august 1970, pp 295-305.